



SIMULATION AND MEASUREMENT OF VERY FAST TRANSIENT OVER VOLTAGES IN A 245KV GIS AND RESEARCH ON SUPPRESSING METHOD USING FERRITE RINGS

J. V. G. Rama Rao¹, J. Amarnath² and S. Kamakshaiah³

¹Department of Electrical Engineering, J. N. T. U, Hyderabad, India

²Department of Electrical Engineering, J.N.T.U. College of Engineering, Hyderabad, India

³Department of Electrical Engineering, Vignan College of Engineering, Hyderabad, India

E-Mail: hodeee.bvcecc@gmail.com

ABSTRACT

Very fast transient over voltages are generated during the switching of disconnections in gas insulated substation. Such over voltages can cause malfunctioning of protection circuits and control circuits and also initiates faults and influence on other components such as transformers. The suppression of VFTO (Very fast transient over voltage) is very important in GIS systems. There are some deficiencies in the existing suppressing methods. In this paper new idea for the suppressing VFTO by ferrite is put forward and the computer simulations were conducted on 245KV GIS models with and without ferrite rings and the results are verified with the experimental results. The simulation test results are closely matched with the experimental results so the use of magnetic rings to suppress VFTO is distinctly efficient.

Keywords: GIS, VFTO, switching operation, ferrite rings, disconnectors, transient enclosure voltages.

1. INTRODUCTION

In a Gas insulated substations Very fast transient over voltages (VFTO) are generated during the switching of dis-connectors in 245KV and above voltage level's GIS. VFTO generated in a GIS should be considered as an important factor in the insulation design. For designing a substation it is essential to know the maximum value of VFTO. Moreover, this VFTO in turn generates Transient Enclosure Voltages (TEV) outside the GIS [1]. Hence studies are carried out on estimation of the VFTO and TEV levels. In GIS, Very Fast Transient Over voltages (VFTO) are caused by two ways, due to switching operations, line to enclosure faults and internal insulation flashover. The internal FTO's generated have traveling wave behavior of a surge. Since FTO's have the characteristics of traveling wave, they can change significantly at different points within GIS [2, 3]. These FTO's travel to the external system through enclosures, gas-air bushings, cable joints, current transformers etc. and may cause damage to the outside equipments like high voltage transformers connected to the GIS. FTO's can also lead to secondary breakdown in GIS. Further they may give rise to electro-magnetic interference. Since the contact speed of the dis-connector switches is low, re-striking occurs many times before the interruption is completed. Each re-strike generates VFTO's with different levels of magnitude. Dis-connector Switches (DS) are used primarily to isolate the operating sections of an HV installation from each other as a safety measure. Beyond this, they must also be able to perform certain switching duties, such as load transfer from one bus bar to another or disconnection of bus bar, circuit breaker etc. Step shaped traveling wave generated between the dis-connector switch contacts propagates in both directions, reflecting at the components of GIS, thus resulting in a complex waveform. Flashover to Ground at the dis-connector switches contacts. Failure of electronic control circuits

connected to GIS, because of electromagnetic interference of VFTO [4], Dielectric strength is reduced under VFTO if non-uniform electric field is formed by the particles (mainly metallic). Effect on components such as bushing and transformer. Transient Enclosure Voltage (TEV) on external surface of the sheath. This may cause flashover to near by grounded objects.

For these reasons, VFTO generated in GIS should be considered as an important factor in the insulation design of not only gas insulated components, but the entire substation. The VFTO generated due to switching operation, the breakdown may occur if a sharp protrusion exists within the GIS [5]. The over voltage pattern and the VFTO level changes after the VFTO breakdown. This type of breakdown is known as Secondary Breakdown. This type of breakdown is also possible at the switching contacts during the current interruption. From the insulation design point of view, this new VFTO level and amplitudes of the high frequency components are also important. For designing a substation it is essential to know the maximum value of VFTO. Hence studies are carried out on estimation of the VFTO levels. For this purpose PSPICE can be used. In PSPICE simulation a suitable equivalent circuit is necessary for each component of the substation.

From the above it can be seen that the estimation of magnitudes of VFTO's and suppression of VFTO's are essential for the design of a GIS. This has been the scope of this paper. The suppression of VFTO's is very important. There are some deficiencies in the existing suppressing methods. In this paper, a new method that using magnetic rings suppressing VFTO will be researched. The magnetic rings sheathed on the GIS conductors can damp the traveling wave and accelerate the attenuation of VFTO. The superimposition of the VFTO results many troubles. VFTO can reach a high amplitude and steepness and may cause damage to insulation and



equipment connected so damping of VFTO is very important.

2. MODELING OF 245KV GIS COMPONENTS

Due to the traveling nature of the VFTO the modeling of GIS makes use of electrical equivalent circuits composed by lumped elements and especially by distributed parameter lines, defined by surge impedances and traveling times. The quality of the simulation depends upon surge impedances and traveling times [6], and also on quality of the model of each individual GIS components. In order to achieve reasonable results even

for longer time periods of some micro seconds (or) for very complex GIS structures highly accurate models for each internal equipment and also for components connected to the GIS are necessary. The equivalent circuit parameters are derived from the following calculations.

2.1 Calculation of inductance

The inductance of the bus duct can be calculated by using the formula [8] given below, where r_1, r_2, r_3, r_4 , are the radii of the conductors in the order of decreasing magnitude and 'l' is the length of the section.

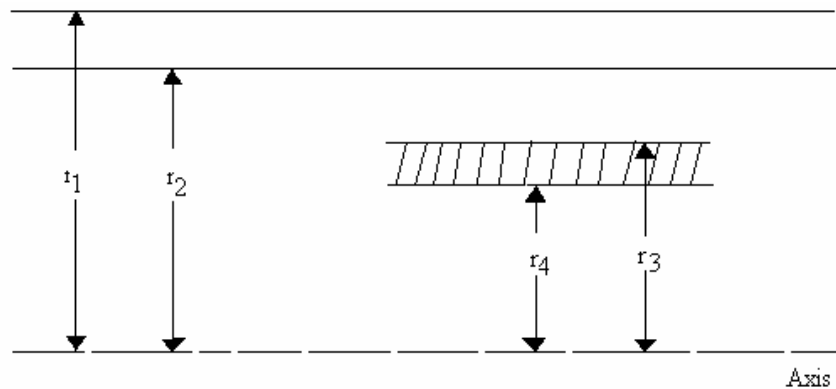


Figure-1. Cross section of typical GIS system.

$$L = 0.001 \times l \times \left[\ln \left(\frac{r_1}{r_3} \right) + \ln \left(\frac{r_2}{r_1} \right) + \ln \left(\frac{r_4}{r_3} \right) + 2 * \frac{\left(\frac{r_2}{r_1} \right)^2}{1 - \left(\frac{r_2}{r_1} \right)^2} * \ln \left(\frac{r_1}{r_2} - 1 \right) \right]$$

2.2 Calculation of capacitance

The Capacitance is calculated with the assumption that the conductors are Cylindrical. Capacitance is calculated by using the standard formulae given below.

$$C = \frac{2 * \pi * \epsilon_0 * \epsilon_r * l}{2.3 * \ln_{10} \left(\frac{b}{a} \right)}$$

Where $\epsilon_0 = 8.854 * 10^{-12}$, $\epsilon_r = 1$

b = Outer cylinder radius

a = Inner cylinder radius

l = Length of the section

2.3 Calculation of capacitance due to spacer

Spacers are used for supporting the inner conductor with reference to the outer enclosure. They are made with Alumina filled epoxy material whose relative permittivity (ϵ_r) is 4. The thickness of the spacer is assumed to be the length of the capacitance for calculation.

2.4 Calculation of variable arc resistance

Based on earlier studies in SF₆ gas, Toepler's Spark Law is valid for calculation of Variable Arc Resistance. The Variable Arc Resistance due to Toepler's formulae [7] is given below:

$$R = \frac{K_T * l}{q_0 + \int_0^t i(t) dt}$$

Where

K_T = Toepler's Constant

= 0.005 volt.sec/mt for SF₆ under Uniform Field conditions

L = Spark Length in meters

q_0 = Initial Charge or Charge at the instant of breakdown

t = Spark Collapse Time in sec.

The value of time varying spark resistance R (t) is calculated until it reaches a value of 1 to 3 ohms. The integral in the denominator sums up the absolute value of current 'i' through the resistance R (t) over the time beginning at breakdown inception. Thus, it corresponds to



the charge conducted through the spark channel up to time 't'.

2.5 Single phase model equivalent circuit for 245KV GIS without ferrite rings

The bus duct is modeled as shown in Figure-2. The GIS bushing is represented by a capacitance of 200pf. A Fixed resistance of 2ohms of the spark channel is connected in series with the circuit breaker. The equivalent circuit is shown in Figure-2 due to trapped charge some

voltage remains on the floating section which can create severe conditions because the first re-strike can occur at the peak of power frequency voltage giving a voltage of 2 p.u. On re-strike the voltages on each side will collapse initially zero and hence creating two 1p.u voltage steps of opposite polarities. In this, it is assumed that re-striking is created at 1p.u and -1p.u respectively on either side of disconnector Switch (DS). The transients due to different switching operations are observed.

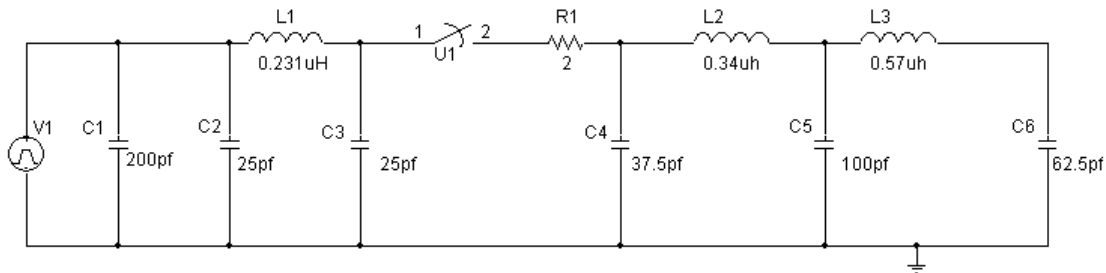


Figure-2. Single-phase equivalent circuit for GIS due to switching operation without ferrite rings.

3. MODELING OF FERRITE RING RINGS

3.1 The ferrite parameters

Ferrite material has different characteristics of saturation magnetic conductivity, frequency response and loss. These characteristics influence the VFTO suppression effect [7].

3.1.1 Magnetic conductivity and frequency response

Magnetic conductivity includes initial magnetic conductivity, the maximal magnetic conductivity and differential magnetic conductivity. This parameter is complex and nonlinear. The suppressing effect on VFTO is determined by equivalent inductance of magnetic ring that relate to the size and the magnetic conductivity of ferrite ring [8]. For the space limiting, the magnetism conductivity should be big enough. On the other hand, the electromagnetic loss of the ferrite ring can be known from the following equation,

$$\frac{P}{V} = \frac{1}{\sqrt{2}} \mu_h H^3 f \tag{1}$$

magnetic hysteresis coefficient, magnetization frequency, volume of ferrite ring and the power of magnetic hysteresis loss. The suppressing effect on the VFTO could be improved by the high Here H, h, f, p, v magnetic strength, magnetic conductivity and frequency. When the effect of the reflect wave and the line loss is eliminated, the voltage of the of bus bar is

$$V_{bus} = E \left\{ 1 - \frac{R_h}{Z + R_h} e^{\left(\frac{Z R_h}{L_d Z + R_h} \right) t} \right\} \tag{2}$$

3.2 Losing characteristic

The magnetic ring fixed on GIS conductive bar should have no influence on the work frequency electric current and the most loss of the ferrite ring produces at high frequency. So the energy of VFTO can be absorbed. The loss of unit volume of ferrite material is

$$P = P_e + P_h + P_c \tag{3}$$

Here $P_e = \epsilon B_{max}^2 f$, $P_h = W_h f$ and P_c is respectively the loss of vortex, hysteresis and remanence. The total power loss can be expressed

$$P = k f^m B^n \tag{4}$$

K = The constant; f = frequency; B = The magnetism flux density; n and m = The index. With equation (4), it can be known that power loss of magnetic ring is in direct proportion to f and B. And it can be know that the loss of the ferrite also has direct proportion relations with the conductivity of magnetism by equation (1).

3.3 The size estimating for ferrite

Mn-Zn ferrite is chosen as its high magnetic saturation, B_s , $B_s \geq 470mT$ (25°C). With the increase of frequency more than 100 kHz, its power loss increases rapidly.

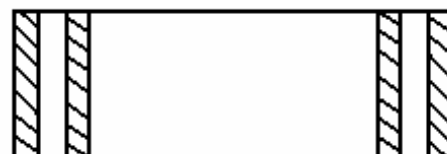


Figure-3. Ferrite ring model.



Different ferrite ring can be equivalent to simply form with uniformity magnetic field. It can be similar to a thin ring dr. The size of the ferrite ring is shown as Figure-4. Different magnetic field line length and ferrite ring section can be expressed with one equivalent length L_e and area A_e . the total magnetic field go through the each section, the equivalent inductance L_i is

$$L_i = \mu_0 \mu_i N^2 \tag{5}$$

and equivalent resistance R_h

$$R_h = hf \frac{L_i}{IN} \tag{6}$$

Here μ_i is the relative initial magnetic conductivity, h is the magnetic hysteresis coefficient, and N is the number of rings. The ferrite ring is composed of lot of ideal thin rings dr

So $IN = 2\pi rH$, and the section area as $dA = adr$.

then the differential inductance is $dL(r) =$

$$\frac{Nd\phi}{I} = N^2 \frac{d\phi}{H2\pi r} = N^2 \frac{Badr}{H2\pi r} \tag{7}$$

from $B = \mu_0 \mu_i H$, the initial differential inductance is

$$dL_i(r) = \mu_0 \mu_i N^2 \frac{a}{2\pi r} \tag{8}$$

Add up all the thin rings, the inductance of ferrite ring is

$$L_i = \mu_0 \mu_i N^2 \frac{a}{2\pi} \ln \frac{r_a}{r_i} \tag{9}$$

Using the similar method, the resistance is

$$R_h = hf L_i NI \frac{1}{\ln \frac{r_a}{r_i}} \tag{10}$$

The L_e and area A_e can be obtained from (5), (6), (9) and (10) as

$$L_e = \frac{2\pi \ln \frac{r_a}{r_i}}{\frac{1}{r_i} - \frac{1}{r_a}} \tag{11}$$

$$A_e = \frac{a \left(\ln \frac{r_a}{r_i} \right)}{\frac{1}{r_i} - \frac{1}{r_a}} \tag{12}$$

Because of the high frequency character of the ferrite ring, fixing it on the GIS conductor bar is equivalent to connecting impedance and inductance between the switch and bus bar. As the Figure-4 shows, R_h and L_i are the equivalent resistance and inductance of the ring and Z is the wave impedance of the bus bar.

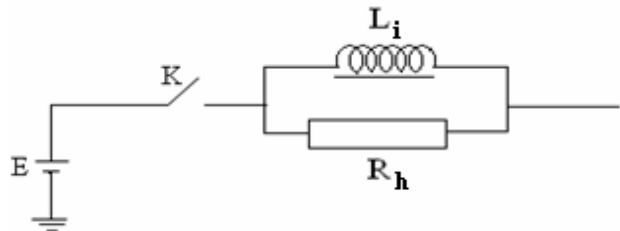


Figure-4. Equivalent circuit of the ferrite ring.

The initial magnetic conductivity μ_i of Mn-Zn ferrite is between 2000 and 10000, and its magnetic hysteresis scale h/μ_i^2 is about 0.1×10^{-8} m/A. It is estimated that the suppressive effect on the VFTO is calculated using above expressions are R_h is 70Ω and L_i is $0.02mH$. The Figure-5 shows the single phase equivalent of the GIS with ferrite rings. The VFTO waveforms for various operations are given in Figure-6 to Figure-9.

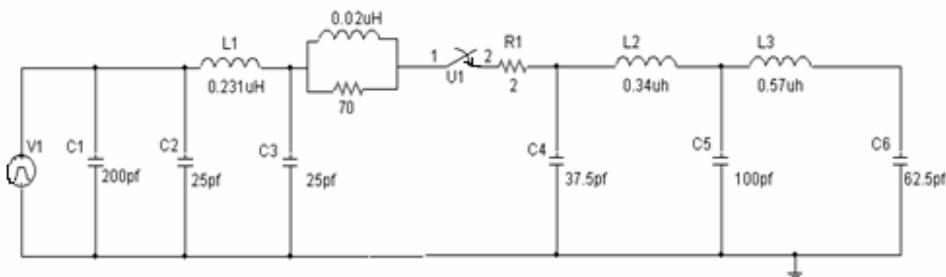


Figure-5. Single- phase equivalent circuit for 245KV GIS due to switching operation with ferrite rings.

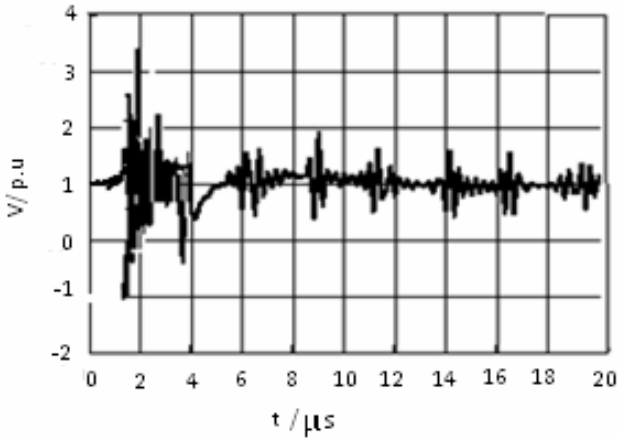


Figure-6. VFTO Wave form for opening operation of DS without ferrite rings.

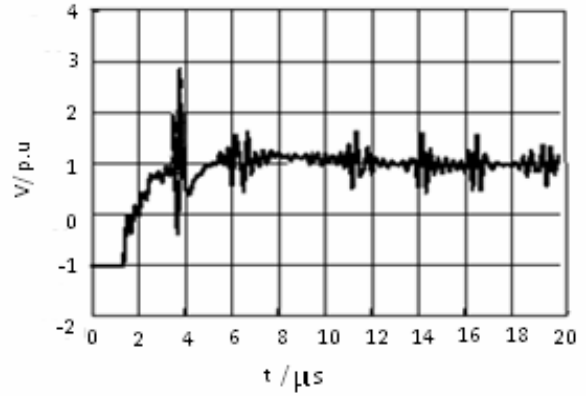


Figure-8. VFTO Wave form for closing operation of DS without ferrite rings.

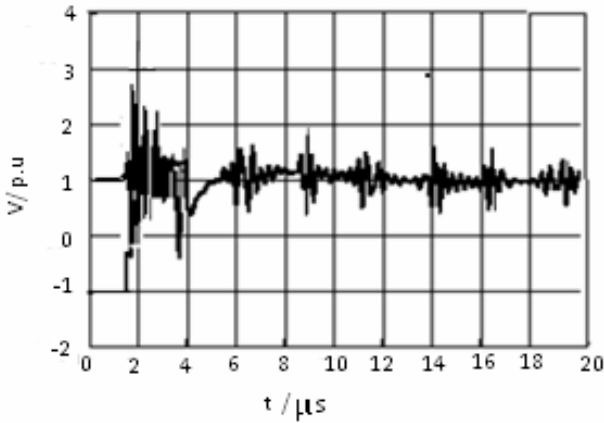


Figure-7. VFTO Wave form for opening operation of DS with ferrite rings.

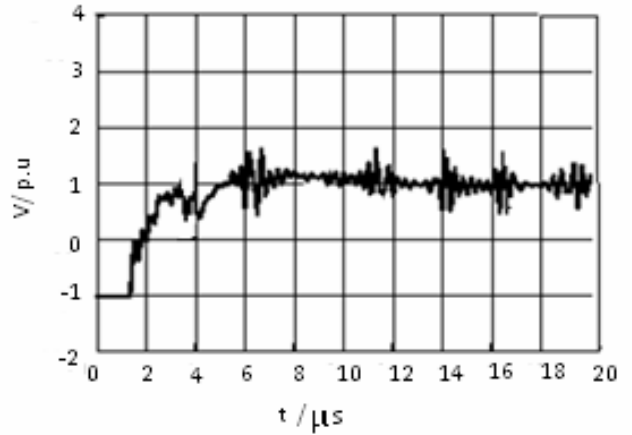


Figure-9. VFTO Wave form for closing operation of DS with ferrite rings.

NOTE: 245KV= 1PU

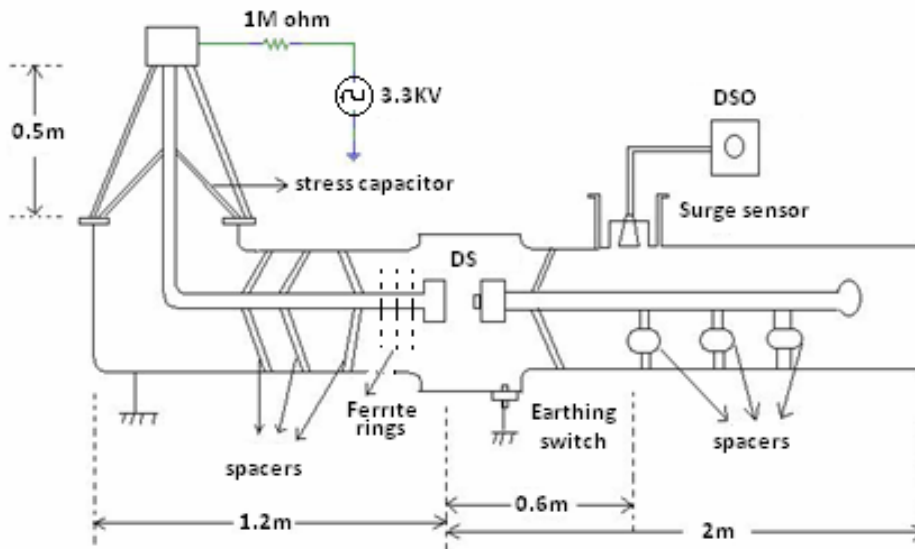


Figure-10. 3.3KV Gas insulated bus duct with dis-connector switch.



4. EXPERIMENTAL RESULTS

In order to know the damp effect on VFTO and to verify validity of the modeling and simulation a low voltage experiment was performed. The experimental investigations of the transient over voltages during disconnector switch operation both closing and opening conditions are considered in this work. The transient over voltages have been measured near the disconnector switch by means of the digital storage 500 MHz sampling rate "Falcon" Digital storage oscilloscope with sample rate 1GS/s and surge sensor. Here two situations are considered i.e. measurements have been carried out on 3.3kv bus duct to measure the VFTO without ferrite rings and with ferrite rings. The variation in the VFTO waveform is shown in Figure-11(a) and Figure-11(b).

The apparatus has a disconnector with an earthing switch, four disk-type spacers, a load bus bar about 4.2m long with three post-type spacers and a 3.3KV gas bushing containing stress capacitor. Further, holding the load side bus bar at zero potential, ac voltage was applied from the high voltage ac power supply to the bushing via a 1 MΩ resistor and VFTO waveform of the closing operation was observed. The ac voltage applied was positive and moving contact of the disconnector was located on the load side. The Figure-11(a) and Figure-11(b) shows the VFTO measurements during DS operation with and without ferrite rings.

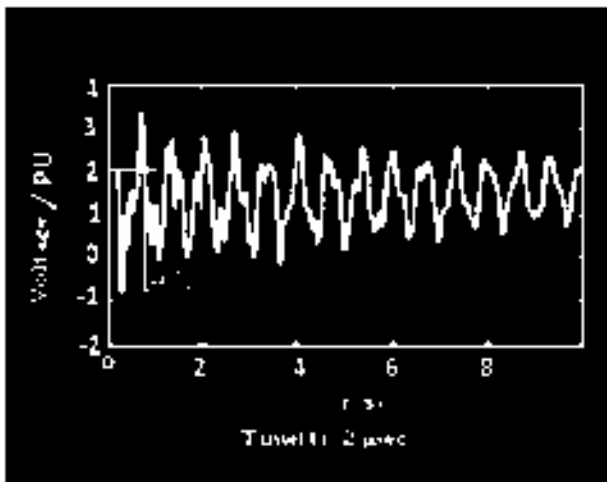


Figure-11(a). Measured VFTO waveform during Closing operation of disconnector switch with out ferrite rings.

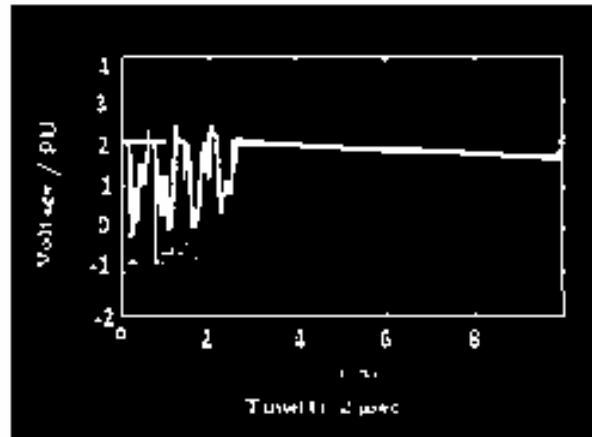


Figure-11(b). Measured VFTO waveform during operation of disconnector switch with ferrite rings.

5. RESULTS

The simulations have been made for the 245KV GIS model, the sketch of which is presented in Figure-5. The transients caused by both opening and closing operation of the disconnector switch (DS) have been determined by using the computer program PSPICE. Time step used by calculations was 0.2ns due to the limited space; the paper presents only a few of the numerous results of the numerical simulations. Figure-6 & 7 shows the transient voltage caused by opening operation of DS. It has been observed that close to the switching point, VFTO waveform has steeper front and higher frequency of oscillation as compared to further away from observation point. During opening of the DS, the maximum possible value of VFTO level is about 3.26 p.u in the case of 245KV GIS has been observed. Similarly the peak value of 2.8 p.u is observed during opening operation of the DS. In the next case the equivalent circuits for ferrite rings have been included in the simulation circuit, the following observations are made from this. Figures 8 and 9 shows peak values of VFTO during closing operation of DS is about 2.8 p.u and it is 1.4 p.u during operation of D.S, the damping effect of VFTO is verified with the experimental results. It is observed that the VFTO peak decreases after insertion of ferrite rings in the equivalent circuit of a 245KV GIS. The suppressing of VFTO is obtained with ferrite rings.

**Table-1.** Comparison of simulation results and experimental results during switching operation of dis-connector switch.

Results	Type of operation	Without ferrite rings		With ferrite rings	
		Voltage (p.u)	Rise time (μ sec)	Voltage (p.u)	Rise time (μ sec)
Simulation results	During closing operation of dis-connector switch	3.4	1.9	2.7	1.6
	During opening operation of dis-connector switch	2.7	3.8	1.4	5
Experimental results	During closing operation of dis-connector switch	3.1	1.5	1.9	1.2
	During opening operation of dis-connector switch	2.9	1.8	1.6	1.3

6. DISCUSSIONS

The simulation of a 245KV GIS has been done for the VFTO estimation during dis-connector switch operation here two situations were considered i.e. simulation of GIS with ferrite rings and without application of ferrite rings. It has been observed that peak magnitude is reduced by 48% during opening operation of DS and 59% during closing operation of DS. The damping effect of VFTOS are verified with experimental results by connecting ferrite rings from the experimental results the VFTO level is reduced by 54% during opening operation of DS 62% during closing operation DS. On the other side magnetic saturation is most important characteristics of ferrite rings. Because of the saturation magnetism flux density. Magnetic saturation is most important characteristics of ferrite rings. Because of saturation magnetism flux density B_s is inversely proportional to temperature i.e. B_s will decrease with the temperature increasing. In the low voltage simulation tests, the temperature changes less for small current magnitudes and B_s cannot get saturated, the VFTO suppression effect is well. However in the GIS of UHV, the equivalent current of VFTO travelling waves can reach to 10^4 A/m. B_s will decrease when the temperature increases. This makes high magnetism soft ferrite material very easy to be saturated and when it is saturated then there will be no much damping effect on VFTO. So it is important for the ferrite rings with large value of flux density (B_s). Further an attempt can be made to verify the damping of VFTO with the ferrite rings having different values of B_s .

7. CONCLUSIONS

The fast transient over voltages that are obtained due to switching operations in GIS are simulated and validity of the results are verified with the experimental results. In this work an attempt is made to reduce the amplitudes of VFTO'S using ferrite rings. The Steepness and maximum peak of the transient over voltages are reduced with application of ferrite rings is observed. The fast transient over voltages can be reduced by 60% with use of ferrite rings to bus duct. It is observed that the peak magnitudes are 26% to 30% higher in case of dis-connector switch closing operation. With effective design and use of the same can effectively reduce the steepness and maximum peak of VFTO generated. The simulation result has diversity with the experimental results this is

because some parameters have ignored. To remove diversity further research on GIS equipment to perfect the model should be carried out. However, these simulations are helpful for an effective shielding of the control circuits within GIS against transient voltages.

REFERENCES

- [1] J. Meppelink, K. Diederich, K. Feser and P. Pfaff. 1989. Very Fast Transients in GIS. IEEE Trans. Power Delivery. 10(1): 223-233.
- [2] Amir Mansour Miri and Zlatan Stojkovic. 2001. Transient Electromagnetic Phenomena in the Secondary Circuits of Voltage and Current Transformers in GIS (Measurements and Calculations). IEEE Trans. Power Delivery. 16(4): 571-575.
- [3] D.E. Thomas, C.M. Wiggins, T.M. Salas, F.S. Nickel and S.E. Wright. 1994. Induced Transients in Substation Cables: Measurements and Models. IEEE Trans. Power Delivery. 9(4): 1861-1868.
- [4] C.M. Wiggins and SE Wright. 1991. Switching transient fields in substations. IEEE Trans. Power Delivery. 6(2): 591-600.
- [5] C.M. Wiggins, D.E. Thomas, F.S. Nickel, T.M. Salas and S.E. Wright. 1984. Transient Electromagnetic Interference in Substations. IEEE Trans. Power Delivery. 9(4): 1869-1884.
- [6] S. Nishiwaki, K. Nojima, S. Tatara, M. Kosakada, N. Tanabe and S. Yanabu. 1995. Electromagnetic Interference with Electronic Apparatus by Switching Surges in GIS - Cable system. IEEE Trans. Power Delivery. 19(2): 739-746.
- [7] M. Mohana Rao, M. Joy Thomas and B.P. Singh. 2002. Frequency Spectrum Analysis of Fast Transient Currents (FTC) during Switching Operation in a 245 kV GIS. IEEE/PES T and D Conference, Japan. pp. 2239-2243.



www.arpnjournals.com

- [8] P. Osmokrovic, S. Krstic, M. Ljevak and D. Novakovic. 1992. Influence of GIS Parameters on the Toepler Constant. IEEE Trans. Electrical Insulation. 27(2): 214-220.
- [9] S. Yanabu, H. Murase, H. Aoyagi, H. Okubo and Y. Kawaguchi. 1990. Estimation of Fast Transient Overvoltage in Gas Insulated Substation. IEEE Trans. Power Delivery. 5(4): 1875-1882.
- [10] Masatake Kawada, Ampol Tungkanawanich, Zen-Ichiro Kawasaki and Kenji Matsu-ura. 2000. Detection of Wide-Band E-M Signals Emitted from Partial Discharge occurring in GIS using Wavelet Transform. IEEE Trans. Power Delivery. 15(2): 467-471.